



## RESEARCH ARTICLE

# DUOX2 regulates secreted factors in virus-infected respiratory epithelial cells that contribute to neutrophil attraction and activation

Dacquin M. Kasumba<sup>1,2</sup> | Sandrine Huot<sup>3,4</sup> | Elise Caron<sup>1</sup> | Audray Fortin<sup>1</sup> |  
 Cynthia Laflamme<sup>4</sup> | Natalia Zamorano Cuervo<sup>1</sup> | Felix Lamontagne<sup>1</sup> |  
 Marc Pouliot<sup>3,4</sup>  | Nathalie Grandvaux<sup>1,2</sup> 

<sup>1</sup>Centre de recherche du Centre Hospitalier de l'Université de Montréal, Montréal, Québec, Canada

<sup>2</sup>Department of Biochemistry and Molecular Medicine, Faculty of Medicine, Université de Montréal, Montréal, Québec, Canada

<sup>3</sup>Département de Microbiologie-Infectiologie et Immunologie, Faculté de Médecine de l'Université Laval, Centre de Recherche du CHU de Québec-Université Laval, Québec City, Québec, Canada

<sup>4</sup>Axe maladies infectieuses et immunitaires, Centre de Recherche du CHU de Québec – Université Laval, Québec City, Québec, Canada

## Correspondence

Marc Pouliot, CRCHU de Québec – Université Laval, 2705 boulevard Laurier, Bureau T1-49, Québec City, QC G1V 4G2, Canada.  
 Email: [marc.pouliot@crchudequebec.ulaval.ca](mailto:marc.pouliot@crchudequebec.ulaval.ca)

Nathalie Grandvaux, CRCHUM, 900 rue St Denis, Bureau R.05.436B, Montréal, QC H2X 0A9, Canada.  
 Email: [nathalie.grandvaux@umontreal.ca](mailto:nathalie.grandvaux@umontreal.ca)

## Present address

Dacquin M. Kasumba, Molecular Biology Laboratory, Department of Basic Sciences, Faculty of Medicine, Université de Kinshasa, Kinshasa, Democratic Republic of Congo

Dacquin M. Kasumba, Laboratory of Clinical Immunology, Institut National de Recherche Biomédicale, Kinshasa, Democratic Republic of Congo

## Funding information

FRQ | Fonds de Recherche du Québec - Santé (FRQS), Grant/Award Number: 295847; Gouvernement du Canada |

## Abstract

The first line of defense against respiratory viruses relies on the antiviral and proinflammatory cytokine response initiated in infected respiratory epithelial cells. The cytokine response not only restricts virus replication and spreading, but also orchestrates the subsequent immune response. The epithelial Dual Oxidase 2 (DUOX2) has recently emerged as a regulator of the interferon antiviral response. Here, we investigated the role of DUOX2 in the inflammatory cytokine response using a model of A549 cells deficient in DUOX2 generated using Crispr-Cas9 and infected by Sendai virus. We found that the absence of DUOX2 selectively reduced the induction of a restricted panel of 14 cytokines and chemokines secreted in response to Sendai virus by 20 to 89%. The secreted factors produced by epithelial cells upon virus infection promoted the migration, adhesion, and degranulation of primary human neutrophils, in part through the DUOX2-dependent secretion of TNF and chemokines. In contrast, DUOX2 expression did not impact neutrophil viability or NETosis, thereby highlighting a selective impact of DUOX2 in neutrophil functions. Overall, this study unveils previously unrecognized roles of epithelial DUOX2 in the epithelial-immune cells crosstalk during respiratory virus infection.

Dacquin M. Kasumba and Sandrine Huot should be considered joint first authors.

Marc Pouliot and Nathalie Grandvaux should be considered joint senior authors.

This is an open access article under the terms of the [Creative Commons Attribution-NonCommercial-NoDerivs](https://creativecommons.org/licenses/by-nc-nd/4.0/) License, which permits use and distribution in any medium, provided the original work is properly cited, the use is non-commercial and no modifications or adaptations are made.

© 2023 The Authors. *The FASEB Journal* published by Wiley Periodicals LLC on behalf of Federation of American Societies for Experimental Biology.

Canadian Institutes of Health Research (IRSC), Grant/Award Number: MOP-137099 and III-134054

## KEYWORDS

antiviral, cytokines, DUOX2, epithelial cells, inflammation, neutrophils, redox, respiratory, virus

## 1 | INTRODUCTION

Human respiratory virus infections are associated with high morbidity and mortality that represent a heavy global health burden.<sup>1,2</sup> Most respiratory viruses that affect humans have a genome composed of RNA.<sup>3</sup> They primarily infect and replicate in respiratory epithelial cells (ECs) along the respiratory tract, which constitute a physical barrier to the outside environment. ECs are equipped with pathogen recognition receptors that sense RNA viruses to trigger the earliest events of the innate host defense via secretion of mucus and soluble mediators. Among the latter, cytokines and chemokines are major determinants of the outcome of the infection and host recovery.<sup>4</sup> ECs secrete antiviral type I and type III interferons (IFN), which through autocrine and paracrine actions limit virus replication and spreading. They also secrete a broad panel of proinflammatory cytokines and chemokines involved in the recruitment and activation of leukocytes in the airway mucosa.<sup>5,6</sup> The capacity of respiratory RNA viruses to modulate the rate, magnitude, and quality of antiviral and proinflammatory responses is associated with the severity of the pathogenesis. Specifically, they are known to antagonize the antiviral IFN response, while inducing an exaggerated proinflammatory response often characterized by an accumulation of neutrophils in the airway tract.<sup>7-9</sup> Therefore, the understanding of the innate responses of infected ECs and how they mediate leukocytes recruitment to the airway mucosa is key.

Reactive oxygen species (ROS) of various sources regulate multiple aspects of virus-host interactions, including virus replication, host defense and pathogenesis.<sup>10-12</sup> NADPH oxidases (NOX1-5, DUOX1-2) produce intracellular and extracellular superoxide and hydrogen peroxide (H<sub>2</sub>O<sub>2</sub>) in various organisms. The distinct isoforms that are widely expressed in various tissues play a role in a broad range of cellular processes,<sup>12,13</sup> including host defense, acid production, fluid homeostasis, regulation of mucin expression, and cell death. ROS produced by NADPH oxidases are increasingly appreciated as critical regulators of the innate antiviral response in the respiratory tract.<sup>12-18</sup> The expression of the DUOX2 isoform, and its maturation factor DUOXA2, was shown to be highly upregulated and the most abundant source of regulated amount of H<sub>2</sub>O<sub>2</sub> in respiratory ECs in response to various RNA viruses, including influenza virus (IAV), respiratory syncytial virus (RSV), rhinovirus, Sendai virus (SeV).<sup>14,15,17,19-23</sup> DUOX2 was also

found among the top 10 most upregulated metabolic genes in SARS-CoV-2-infected ECs.<sup>22</sup> The *DUOX2/DUOXA2* gene induction was found to result from the synergistic action of IFN $\beta$  with TNF or IL1 $\beta$ .<sup>15,17</sup> Compelling evidence has implicated DUOX2 in various aspects of the innate antiviral response. Notably, DUOX2 contributes to the increased expression of pathogen recognition receptors.<sup>24</sup> Additionally, we and others have shown that extracellular H<sub>2</sub>O<sub>2</sub> produced by DUOX2 restricts SeV, RSV, and IAV replication in part through a positive feed-back regulation on IFN $\beta$  and IFN $\lambda$  levels.<sup>15,16</sup> Furthermore, intranasal administration of DUOX2-encoding DNA in mice reduced IAV replication in the airways.<sup>25</sup> In the present study, we aimed to determine whether DUOX2 also contributes to the regulation of the inflammatory arm of the cytokine response mounted by ECs in response to virus infection.

Using DUOX2-deficient A549 cells generated through Crispr/Cas9-mediated genomic modification, we unveiled a selective role of DUOX2 in the induction of a selected group of secreted cytokine and chemokine levels during infection by the respiratory virus, SeV. Soluble mediators secreted by infected ECs were found to contribute to the activation of the innate immune response through the enhancement of neutrophils chemotaxis, NETosis and expression of markers of adhesion and degranulation. We demonstrate that SeV-infected ECs drive neutrophil attraction and activation, in part through the DUOX2-dependent secretion of TNF and chemokines. Altogether, these findings point to previously unrecognized roles of epithelial DUOX2 in the epithelial-immune cells crosstalk during respiratory virus infection.

## 2 | MATERIAL AND METHODS

### 2.1 | Reagents

Dextran-500, adenosine deaminase (ADA) and catalase from bovine liver were from Sigma-Aldrich, Oakville, ON, Canada. R7050, AZD5069, AMG487, Cenicrivoc, Phorbol 12-myristate 13-acetate (PMA) were from Cayman Chemical, Ann Arbor, MI, USA. Calcein-AM and SYTOX green were from Invitrogen, Eugene, OR, USA. Anti-human G-CSF and recombinant IFN $\beta$  and TNF were from R&D Systems, Minneapolis, MN, USA. Anti-human GM-CSF was from Biolegend, San Diego, Ca, USA. Human immunoglobulins (IgGs) were from

Innovative Research, Inc., Novi, MI, USA. Human Fc-Block, BV421-labeled mouse anti-human CD35 (Clone E11), APC-labeled mouse anti-human CD11b (Clone ICRF44), PE-labeled mouse anti-human CD63 (Clone H5C6), FITC-labeled mouse anti-human CD66b (Clone G10F5) and PerCP-Cy<sup>TM</sup>5.5-labeled mouse anti-human CD16 (Clone 3G8) were all from BD Biosciences, San Jose, CA, USA. General chemicals were from Bioshop, Burlington, ON, Canada.

## 2.2 | Generation of A549 cells deficient in DUOX2

A549 cells (American Type Culture Collection, ATCC) and derivatives were grown in Ham F12 medium (GIBCO) supplemented with 1% L-Glutamine (GIBCO) and 10% heat-inactivated Fetalclone III serum (HI-FCI-III, Hyclone) at 37°C and 5% CO<sub>2</sub>. Cultures were tested negative for mycoplasma contamination (MycoAlert Mycoplasma Detection Kit, Lonza) every 2 months. For generation of A549 deficient in DUOX2 (A549-DUOX2<sup>Def</sup>) and control cells (A549-Ctrl), A549 cells were seeded in a 12-well plate for co-transfection with 1.6 µg of Cas9 Nuclease Expression Plasmid (Dharmacon, #U-005200-120), 50 nM TracrRNA (Dharmacon, #U-002000-20) and 50 nM crRNA specific to either exon 4 of human DUOX2 (Gene ID: 50506; sequence: ATACACACCGTCGGCGTAAT) or non-targeting control (Dharmacon, #U-007501-05 and #U-007502-05) using 40 µg/ml Dharmafect DUO transfection reagent (Dharmacon, #T-2001-02). After 48 h, 2 µg/ml puromycin (Sigma-Aldrich) was added to select for Cas9 expression plasmid and culture was pursued for 7 days. Monoclonal populations were obtained by seeding 40 cells/15 cm plates followed by isolation of clones using cloning rings. Gene editing was confirmed by Sanger sequencing at the Génome Québec Innovation Centre (McGill University, Montréal, QC). CRISP-ID web application tool was used to locate the targeted region and monitor the insertions/deletions within the gene. Lack of expression of DUOX2 was confirmed by immunoblot.

## 2.3 | Cell infection and treatment

Subconfluent A549-Ctrl or A549-DUOX2<sup>Def</sup> cells were infected with SeV (Cantell strain, Charles River Laboratories) at 40 hemagglutinin units (HAU)/10<sup>6</sup> cells in serum free Ham F12 medium (SFM) containing 1% Glutamine for the first 2 h before addition of 10% HI-FCI-III. The infection was pursued for the indicated time. For cytokine stimulation, cells were treated with

recombinant IFNβ or TNF at 1000 U/ml and 10 ng/ml, respectively, in Ham F12 medium containing 1% glutamine and 2% HI-FCI-III (F12-2%HI-FCI-III) for the indicated times.

## 2.4 | Protein extraction and Immunoblots

For analysis of signaling pathways, cells were harvested in cold dPBS (GIBCO), pelleted by centrifugation at 16 200g for 30 s and resuspended in pre-chilled lysis buffer composed of 50 mM Hepes pH 7.4, 150 mM NaCl, 5 mM EDTA, 10% glycerol, and 1% IGEPAL (Sigma-Aldrich) completed with 1 µg/ml of leupeptin, 2 µg/ml of aprotinin, 5 mM of sodium fluoride, 1 mM of activated Na<sub>3</sub>VO<sub>4</sub>, 2 mM of p-nitrophenyl phosphate, and 10 mM b-Glycerophosphate pH 7.5. After incubation on ice for 20 min and three freeze/thaw cycles, lysates were clarified at 16 200g for 20 min at 4°C. The supernatant was isolated and used as the whole cell extract (WCE). Quantification of proteins was performed using a Bradford assay (Biorad). Thirty micrograms of WCE were resolved by electrophoresis on SDS-PAGE and immunoblotted on a nitrocellulose membrane according to the method detailed by Robitaille et al.<sup>26</sup> The following primary antibodies were used: anti-IRF-3-phospho-Ser396 (described in Servant et al.<sup>27</sup>), anti-IRF-3 (Active Motif, cat.#39033), anti-P65-phospho-Ser536 (Cell Signaling, cat.#3033), anti-p65 (Santa Cruz, cat.#SC-372), anti-phospho-IκBα-Ser32 (Cell Signaling, cat.#2859), anti-IκBα (Cell Signaling, cat.#9242), anti-phospho-STAT1-Tyr701 (Cell Signaling, cat.#7649), anti-STAT1 (Cell Signaling, cat.#9176), anti-SeV (MBL life Science, cat.#PD029), and anti-actin (clone AC-15, Sigma, cat.#A5441) diluted in either PBS containing 0.5% Tween (MP Biomedicals, PBS-T) completed with 5% Bovine Serum Albumin (Millipore Sigma, cat.# A7906) or 5% milk (Carnation).

For DUOX2 immunoblots, cells were washed with dPBS before addition of chilled dPBS completed at the time of use with 1 mM phenylmethylsulfonyl fluoride (Bioshop, cat. #PMS123.5), 0.01 mM chymostatin (Sigma, cat. #C7268) and 10 µl/ml protease inhibitor cocktail (Sigma-Aldrich, cat. #P8340) directly to the plates. Cells were scraped and sonicated (3 × 20 pulses) on ice. The lysates were centrifuged at 16 200g for 20 min at 4°C. The supernatant was ultracentrifuged at 100 000g in a S120AT3-0172 rotor at 4°C for 30 min. The pellet was resuspended in 125 mM Tris-HCl, 10% Glycerol, 2% SDS containing 1 mM phenylmethylsulfonyl fluoride (Bioshop, cat. #PMS123.5), 0.01 mM chymostatin (Sigma, cat. #C7268) and 10 µl/ml protease inhibitor cocktail (Sigma-Aldrich, cat. #P8340), 0.1 M

dithiothreitol and protein concentration quantified using Protein Quantification RC DC method (Biorad). SDS-PAGE electrophoresis (6.5% acrylamide/bis-acrylamide resolving gel) were conducted immediately using 30 µg of membrane extracts after addition of 1% bromophenol blue. Immunoblots were performed as described above using recombinant anti-NaK ATPase (ABCAM, cat. #AB76020) and anti-DUOX1/2 (obtained from Dr. Miot, Belgium) primary antibodies diluted in PBS-T containing 5% milk.

## 2.5 | Epithelial cell-derived conditioned medium generation

For preparation of EC-derived conditioned medium (Co-SN), A549-Ctrl and A549-DUOX2<sup>Def</sup> cells were left uninfected or infected with SeV in F12-2%HI-FCI-III for 24 h. Where indicated, 400 U/ml catalase was added 4 h before supernatant collection. Supernatants were collected and clarified for 5 min at 1000 g followed by a 10 min centrifugation at 10 000g. Where indicated, Co-SN were treated with UV for 20 min to inactivate SeV.

## 2.6 | Cytokine and chemokine quantification

Cytokine and chemokine quantification was performed on Co-SN by Eve technologies, Calgary, AB, Canada, using Luminex-based human Cytokine multiplex Assays. IFNβ was quantified by ELISA using the Human IFN-beta Quantikine QuickKit ELISA (R&D Systems).

## 2.7 | Human neutrophils isolation and incubation with conditioned medium

The Université Laval ethics committee approved all experiments involving human tissues (2021–5336). Informed consent was obtained in writing from all donors. Data collection and analyses were performed anonymously. Neutrophils were isolated under sterile conditions at room temperature, essentially as described in Fiset et al.<sup>28</sup> Briefly, 200 ml of venous blood on isocitrate anticoagulant solution from healthy volunteers were collected and distributed in 50-ml conical tubes and were centrifuged at 400g for 10 min; resulting platelet-rich plasma was discarded. Leukocytes were obtained following sedimentation of erythrocytes with 10 ml of 2% (w/v) Dextran-500. Neutrophils were separated from other leukocytes by centrifugation at 600g for 20 min on a 10 ml lymphocyte separation medium (Wisent,

St-Bruno, QC, Canada). Contaminating erythrocytes were removed using 20 s of hypotonic lysis. Purified granulocytes (>95% neutrophils, <5% eosinophils, basophils) contained less than 0.2% monocytes. Viability was greater than 98%, as determined by trypan blue dye exclusion. Neutrophils were resuspended ( $10^7$  cells/ml) at 37°C in F12-2%HI-FCI-III and exposed to EC-derived Co-SN. Each experiment was entirely performed with neutrophils from the same donor. Conversely, distinct independent experiments were performed with neutrophils from different donors. In specific experiments, neutrophils were pre-incubated for 30 min at 37°C with 2 µM TNF receptor-I antagonist R-7050, 100 nM CXCR2 antagonist AZD5069, 1 µM CXCR3 antagonist AMG487, or 1 µM CCR2-CCR5 antagonist Cenicrivoc either individually or in combination as indicated. Alternatively, EC-derived Co-SN were pre-treated for 30 min at 37°C with 10 µg/ml anti-G-CSF or anti-GM-CSF neutralizing antibodies before further use.

## 2.8 | Neutrophil viability

Neutrophil viability was assessed using a FITC Annexin V Apoptosis Detection Kit (BD Biosciences). Neutrophils ( $10^7$  cells/ml) were incubated with EC-derived Co-SN diluted 1:1 with F12 medium, for 24 h at 37°C. Samples were centrifuged and resuspended in 100 µl annexin binding buffer. Annexin V and propidium iodide (5 µl each) were added to samples and incubated for 15 min in the dark before the addition of 400 µl of annexin binding buffer. Analysis was performed by flow cytometry using a FACS Canto II flow cytometer with FACSDiva software, version 6.1.3 (BD Biosciences).

## 2.9 | Chemotaxis

Neutrophil chemotaxis was monitored as described in Frevert et al.<sup>29</sup> with modifications. Briefly, neutrophils were resuspended ( $10^7$  cells/ml) in RPMI 1640 containing 10% decompartmented FBS and supplemented with 0.1 U/ml ADA, to prevent accumulation of endogenous adenosine in the medium, thus minimizing its previously demonstrated modulating effects on neutrophils.<sup>30</sup> Neutrophils were incubated with 5 µg/ml calcein-AM for 30 min at 37°C in the dark with agitation, washed twice and resuspended in F12 medium supplemented with ADA at  $5 \times 10^6$  cells/ml. The bottom chamber of ChemoTx 101–5 plates (Neuro Probe, Gaithersburg, MD) was filled with Co-SN diluted 1:1 in F12-2%HI-FCI-III to a total of 31 µl. A polycarbonate filter was positioned in each well and neutrophils were placed on the top (30 µl;  $3 \times 10^6$  cells/ml). Neutrophils were allowed to migrate for 1 h at 37°C and 5% CO<sub>2</sub> in the dark. Non-migrating



neutrophils were removed by gently wiping the filter with a tissue. Total fluorescence from a known number of neutrophils was determined by placing 30  $\mu$ l of each concentration (i.e., 0.125, 0.25, 0.5, 1.0, 2.0, 3.0, and  $5.0 \times 10^6$  neutrophils/ml) in wells of the plate bottom chamber. Cell migration was measured with a microplate fluorescence reader (ex/em: 485/530nm) with bottom-read configuration (FL600; Bio-Tek Instruments, Winooski, VT).

## 2.10 | Measure of neutrophil production of reactive oxygen species

Neutrophil ROS production was measured as previously described in Fossati et al.<sup>31</sup> with modifications. Briefly, Co-SNs (100  $\mu$ l) were placed in 96-well white microplates (BrandTech® Scientific, Inc., Essex, CT, USA). Neutrophils ( $2 \times 10^6$  cells/ml; 100  $\mu$ l) in F12-2%HI-FCL-III supplemented with ADA in the presence of 20  $\mu$ M luminol were added. Samples were incubated at 37°C in the microplate reader Infinite M1000 PRO with i-control 2.0 software (Tecan, Morrisville, NC, USA). Luminescence intensity was monitored every 5 min for 120 min. Heat-aggregated immunoglobulin G (HA-IgG; 1 mg/ml) was used as a positive control for ROS induction.

## 2.11 | Measurement of NET production

NET formation was performed essentially as in Gray et al.<sup>32</sup> with modifications. Briefly, 100  $\mu$ l of Co-SN, or control F12-2%HI-FCL-III, were placed in 96-well white microplates (BrandTech® Scientific, Inc., Essex, CT, USA) before the addition of neutrophils ( $5 \times 10^5$  cells/ml; 100  $\mu$ l) in F12-2%HI-FCL-III supplemented with ADA. Plates were incubated at 37°C, 5% CO<sub>2</sub> for 4 h before the addition of 5  $\mu$ M SYTOX green. NET formation was evaluated by measuring the fluorescence (ex/em: 504/523 nm) in each well after subtraction of the background fluorescence. PMA (10 nM) was used as a positive control.

## 2.12 | Neutrophils surface marker analysis

Following incubation of neutrophils ( $1 \times 10^7$  cells/ml) with Co-SN diluted 1:1 with F12-2%HI-FCL-III for 30 min at 37°C, cells were spun and resuspended in Hank's Balanced Salt Solution (HBSS) containing 10 mM HEPES pH 7.4, 1.6 mM Ca<sup>2+</sup>, no Mg<sup>2+</sup> and human Fc-Block. Cells were incubated with BV421-labeled mouse anti-human CD35, APC-labeled mouse anti-human CD11b, PE-labeled mouse anti-human CD63, FITC-labeled mouse

anti-human CD66b and PerCP-Cy™5.5-labeled mouse anti-human CD16, for 30 min in the dark at 4°C. Samples were fixed with 1% paraformaldehyde before analysis with a FACS Canto II flow cytometer with FACSDiva software, version 6.1.3 (BD Biosciences). The gating strategy is presented in [Figure S1](#).

## 2.13 | Statistical analyses

Statistical comparisons were performed with Prism 8 software (GraphPad) using the indicated tests. *p*-values were considered significant when <0.05.

# 3 | RESULTS

## 3.1 | Epithelial DUOX2 genomic knockdown does not affect key innate immune signaling pathways

In our previous study, we evaluated the contribution of respiratory epithelial DUOX2 in the antiviral response against RNA viruses using an RNA silencing approach.<sup>15</sup> To further study the role of DUOX2, we used a CRISPR-Cas9 approach to generate monoclonal A549 cells deficient in DUOX2 (A549-DUOX2<sup>Def</sup>) as well as the corresponding ctrl cells (A549-Ctrl). Previous data showed that DUOX2 expression is inducible upon virus infection in ECs.<sup>14,15,17,19–23</sup> Infection by SeV induced the expression of DUOX2 in A549-Ctrl cells, but not in A549-DUOX2<sup>Def</sup> cells ([Figure 1A](#)), confirming that the CRISPR-Cas9 editing strategy was successful.

Using these cells, we first assessed the activation of the NF- $\kappa$ B and IRF-3 transcription factors, which have a major role in the regulation of antiviral and proinflammatory cytokine and chemokine encoding genes.<sup>33</sup> DUOX2 knockout did not alter the phosphorylation of IRF-3 and NF- $\kappa$ B induced by SeV infection ([Figure 1B,C](#)). Because NF- $\kappa$ B and STAT1 signaling mediate the expression of immunoregulatory, inflammatory, and antiviral genes induced by TNF and IFN-I produced during virus infection, respectively,<sup>34,35</sup> we next investigated the functionality of these pathways. Phosphorylation of I $\kappa$ B $\alpha$  induced by TNF ([Figure 1D](#)) and of STAT1 triggered by IFN $\beta$  ([Figure 1E](#)), were induced similarly in A549-DUOX2<sup>Def</sup> and A549-Ctrl cells. Together, these data indicate that epithelial DUOX2 is not required for the activation of key signaling cascades involved in the innate immune defense. To mitigate potential clonal effects, the four clones of A549-Ctrl or A549-DUOX2<sup>Def</sup>, respectively, were pooled to generate polyclonal cell lines that were used in subsequent experiments. ([Figure 1F](#)).

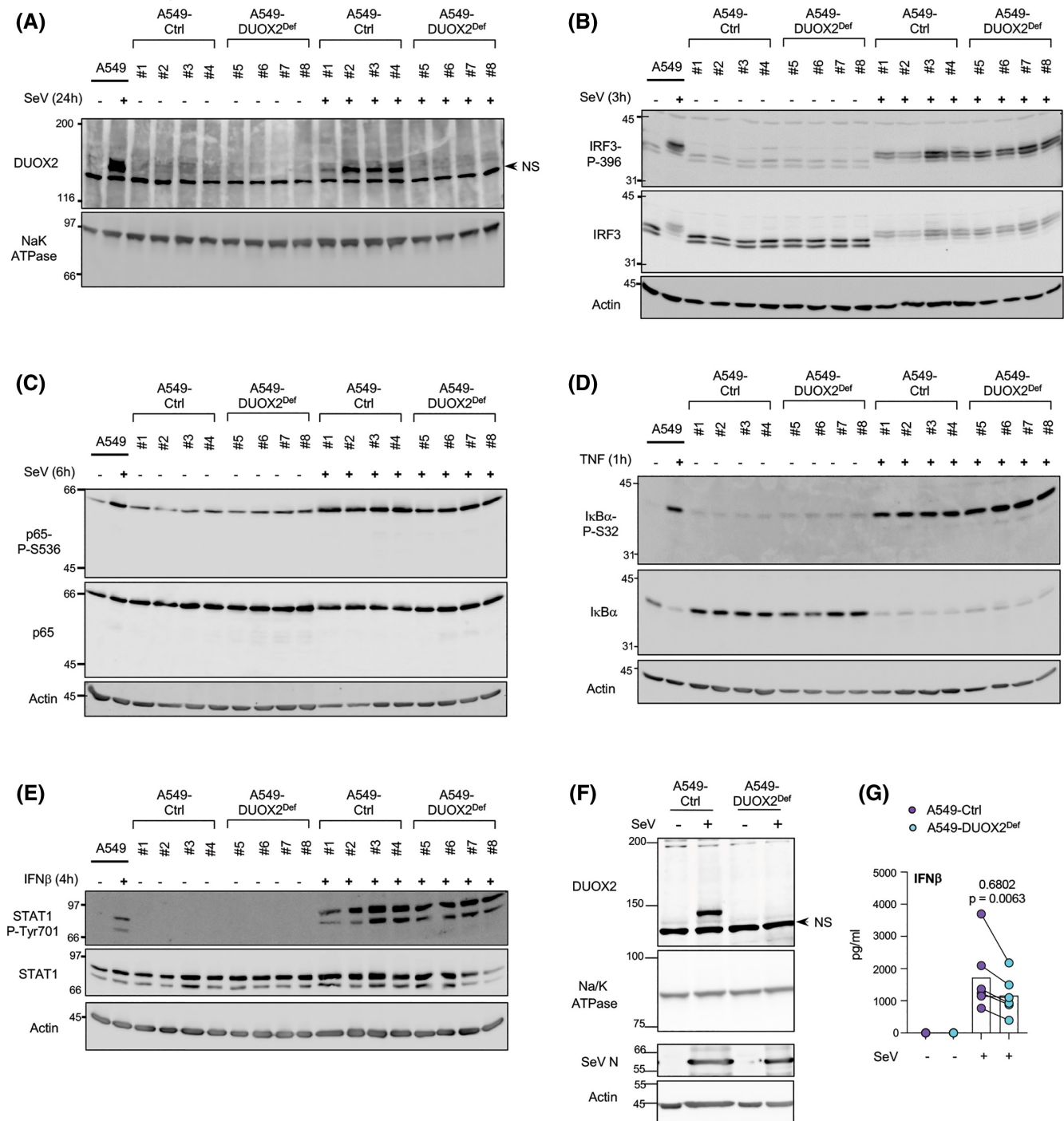


**FIGURE 1** Innate immune signaling in DUOX2-deficient A549 cells infected with Sendai virus. A549 cells were genetically modified using Crispr/Cas9, either with a ctrl gRNA (A549-Ctrl) or DUOX2-targeting gRNA (A549-DUOX2<sup>Def</sup>). Monoclonal cell populations were isolated. In (A–C), A549-Ctrl and A549-DUOX2<sup>Def</sup> clones were infected with SeV (40 HAU/10<sup>6</sup> cells) for the indicated times. In (D), A549-Ctrl and A549-DUOX2<sup>Def</sup> clones were treated with TNF (10 ng/ml) for 1 hr. In (E), clones were treated with IFNβ (1000 U/ml) for 4 h. (F) Pools of A549-Ctrl and A549-DUOX2<sup>Def</sup> clones were pooled and infected with SeV (40 HAU/10<sup>6</sup> cells) for 24 h. In (A and F), Membrane extracts were immunoblotted using a DUOX1/2-specific antibody to monitor DUOX2 protein levels and anti-NaK ATPase antibodies were used as a loading control. In (B–E), WCE were immunoblotted using anti-IRF3-P-Ser396, anti-IRF-3, anti-p65-P-Ser536, anti-p65, anti-IκBα-P-Ser32, anti-IκBα, anti-STAT1-P-Tyr701 and anti-STAT1. Anti-Actin was used as a loading control. (G) A549-Ctrl (violet) and A549-DUOX2<sup>Def</sup> (blue) pools were infected with SeV (40 HAU/10<sup>6</sup> cells) for 24h and the production of IFNβ was quantified by ELISA (*n* = 6 independent experiments). Statistical comparisons were performed using a ratio-paired *t*-test. The geometric mean of ratios and *p*-value are indicated.

### 3.2 | Epithelial DUOX2 shapes the profile of cytokines and chemokines secreted in response to SeV

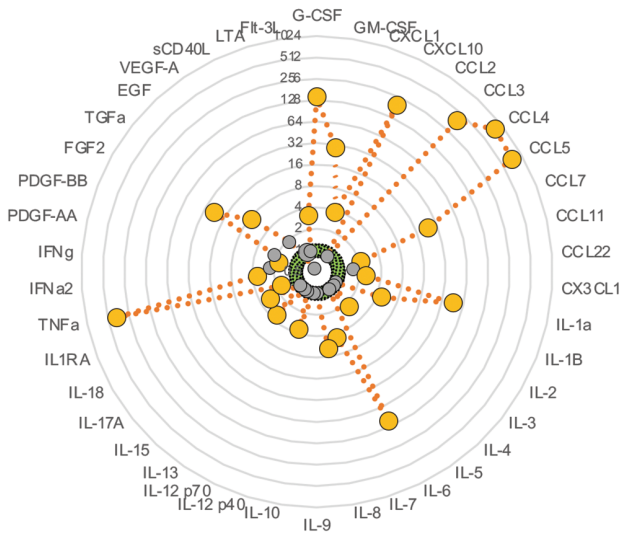
ECs in the respiratory tract secrete a wide range of cytokines and chemokines initiating the recruitment and activation of inflammatory cells upon virus infection.<sup>36,37</sup> We previously documented that DUOX2 in respiratory ECs is required for the sustained production of IFN $\beta$  in response to respiratory RNA viruses.<sup>15</sup> We confirmed in our CRISPR-Cas9 genome-edited model that secreted IFN $\beta$  levels were significantly impaired in A549-DUOX2<sup>Def</sup> infected with SeV compared to control cells (Figure 1G). We then sought to determine if the role of DUOX2 in the modulation of cytokine levels extended beyond IFN $\beta$ . Therefore, we analyzed the supernatant of A549-Ctrl or A549-DUOX2<sup>Def</sup> cells left uninfected or infected cells with SeV for 24 h against a panel of cytokines and chemokines using Luminex-based multiplex assays. Several cytokines and chemokines were significantly induced in SeV-infected A549-Ctrl compared to uninfected cells (Figure 2A,C and Figure S2). Eleven of these cytokines/chemokines, namely G-CSF, GM-CSF, CXCL10, CCL3, CCL4, CCL5, CCL7, IL-1 $\alpha$ , IL-6, TNF, and FGF2, were strongly induced, and stood out with increases of 22.83 to 725.5 folds (Figure 2A,C). The comparison of A549-DUOX2<sup>Def</sup> cells and A549-Ctrl cells showed that the induction of a restricted panel of 14 cytokines/chemokines induced by SeV infection is dependent on the expression of DUOX2. The production of G-CSF, GM-CSF, CXCL1, CXCL10, CCL3, CCL7, IL-1 $\alpha$ , FGF-2, and TNF was most severely impaired in the absence of DUOX2 with a reduction between 86% and 46% compared to control cells, while induction of CX3CL1, IL-1 $\beta$ , IL-4, IL-15, and PDGF-AA was reduced by 20%–40% (Figure 2B,C and Figure S2). Of note, TGF $\alpha$  exhibited an increasing trend in DUOX2-deficient cells (Figure 2B,C), although it remained produced at a very low level (Figure 2B,C). We next sought to determine whether the role of DUOX2 in the regulation of the cytokine and chemokine profile is dependent on H<sub>2</sub>O<sub>2</sub>. We analyzed the levels of some of the DUOX2-dependent cytokines and chemokines in the supernatant of A549-Ctrl cells left uninfected or infected cells with SeV for 24 h in the absence or presence of catalase. We observed a similar trend with catalase than that observed in the absence of DUOX2 providing evidence toward H<sub>2</sub>O<sub>2</sub>-dependent regulation (Figure 3). Overall, our results suggest that DUOX2 deficiency is remodeling the profile of a specific panel of cytokines and chemokines secreted by A549 cells in response to SeV hence hinting at a role of epithelial DUOX2 in the cytokine-driven immune response.

### 3.3 | DUOX2-dependent secreted factors attract human neutrophils and upregulate activation markers

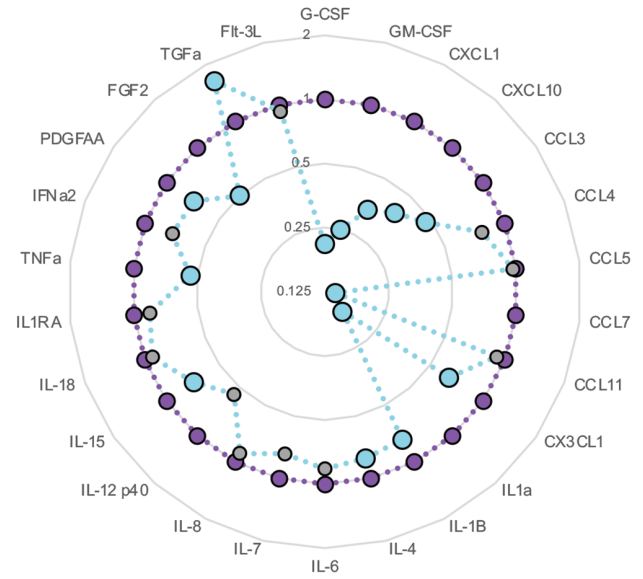
Neutrophilia in the lungs is associated with the pathogenesis of several respiratory viral infections. Epithelium–neutrophil interactions have recently begun to attract interest in understanding the regulation of the innate immune response.<sup>38,39</sup> Analysis of the DUOX2-dependent cytokine profile secreted upon infection of A549 cells with SeV pointed to a potential for regulating neutrophil phenotype. For instance, G-CSF and GM-CSF promote the production and proliferation of neutrophils, while CXCL1, CXCL10, CCL7, CCL3, and TNF, among others, attract neutrophils and promote functions such as adhesion and degranulation.<sup>40–44</sup> Therefore, we sought to evaluate the impact of epithelial DUOX2-deficiency on neutrophils by using an ex-vivo system in which isolated primary human neutrophils are exposed to conditioned media (Co-SN) from either A549-DUOX2<sup>Def</sup> or A549-Ctrl cells left uninfected or infected by SeV (Figure 4A). We then assessed neutrophil viability, chemotaxis, ROS production, formation of extracellular traps (NET), and surface expression of adhesion and degranulation markers.

Regardless of the Co-SN to which neutrophils were exposed, viability after 24 h was similar (Figure 4B), indicating that neither SeV-infection of A549 cells, nor DUOX2-deficiency, impact neutrophil viability within this time frame. On the other hand, Co-SN from infected A549-Ctrl cells (Ctrl-SeV) significantly increased neutrophil chemotaxis compared to Co-SN from uninfected cells (Ctrl-Mock). However, chemotaxis induced by Co-SN from infected A549-DUOX2<sup>Def</sup> cells (DUOX2<sup>Def</sup>-SeV) was significantly lower compared to infected Ctrl cells (Figure 4C), showing that the potential of factors secreted from SeV-infected ECs to attract neutrophils, partially depends on DUOX2. Analysis of ROS production by neutrophils revealed significant induction by Ctrl-SeV Co-SN compared to Ctrl-Mock Co-SN, but the levels were marginal compared to heat-aggregated IgG (HA-IgG), a classic inducer of oxidative burst.<sup>45</sup> While DUOX2<sup>Def</sup>-SeV Co-SN exhibited an apparently stronger ability to stimulate ROS production by neutrophils compared to Ctrl-SeV Co-SN, the levels remained very low (Figure 4D). Ctrl-SeV Co-SN significantly stimulated NETosis compared to Co-SN from uninfected cells although to a modest level compared to PMA, a well-known NET inducer. No significant difference was observed when using Co-SN from A549-DUOX2<sup>Def</sup> cells (Figure 4E), indicating that NETosis induced by secreted factors derived from SeV-infected ECs is not dependent on DUOX2. Finally, we monitored surface markers which provide insights into the adhesion (CD11b), degranulation

(A) ● Ctrl-Mock ● Ctrl-SeV



(B) ● Ctrl-SeV ● DUOX2<sup>Def</sup>-SeV



(C) ● A549-Ctrl ● A549-DUOX2<sup>Def</sup>

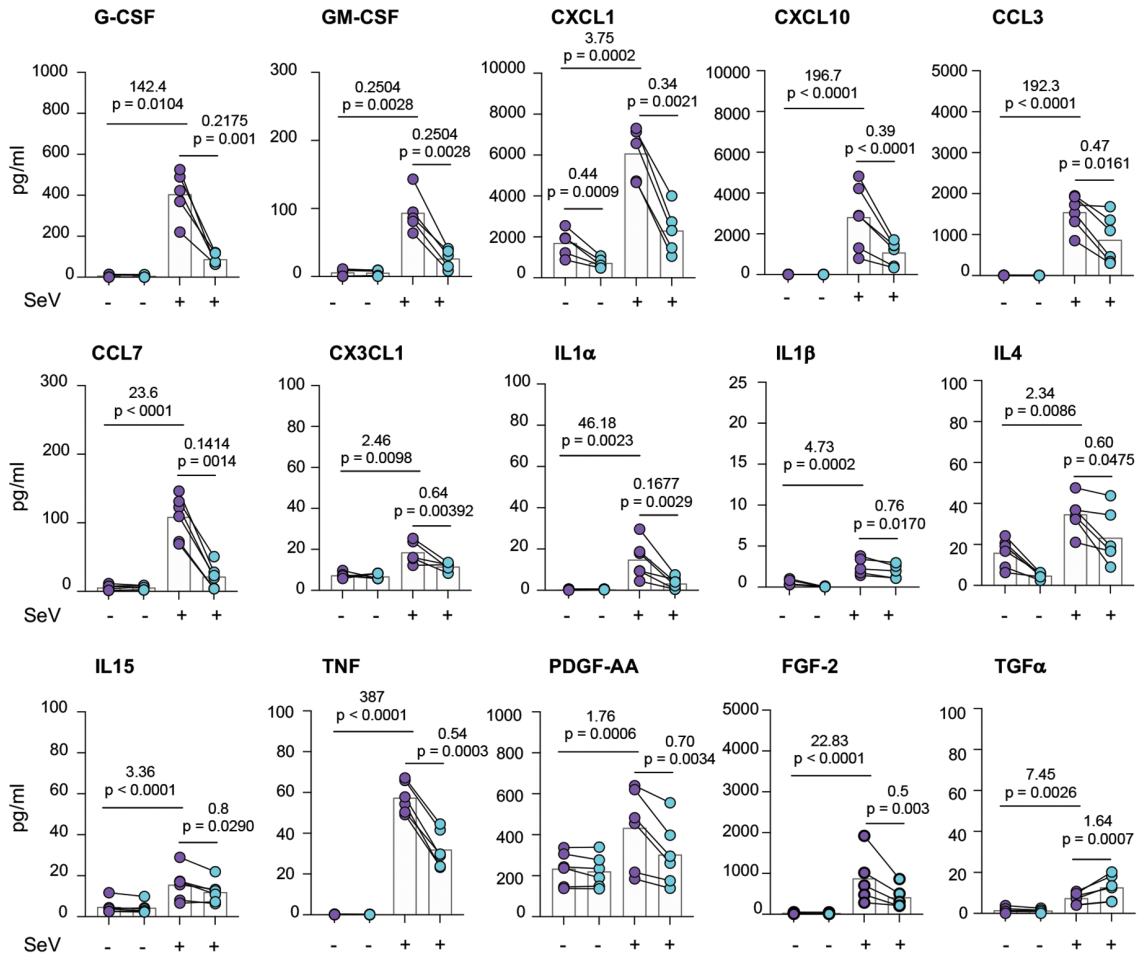




**FIGURE 2** DUOX2 is required for the epithelial expression of a panel of cytokines induced by SeV infection. A549-Ctrl and A549-DUOX2<sup>Def</sup> cells were left uninfected or infected with SeV (40 HAU/10<sup>6</sup> cells) for 24 h and the release of cytokines and chemokines was quantified using Luminex-based multiplex assays. (A) Radar plot of cytokine and chemokine levels in SeV-infected A549-Ctrl (Ctrl-SeV) represented as fold over uninfected A549-Ctrl (Ctrl-Mock) condition (green). Cytokines significantly induced ( $n \geq 4$ ;  $p < 0.05$ ) are represented in yellow. Non-significant variations are shown in gray. (B) Radar plot of cytokine levels in A549-DUOX2<sup>Def</sup> infected with SeV (DUOX2<sup>Def</sup>-SeV) represented as fold over SeV-infected A549-Ctrl (Ctrl-SeV) condition (violet). Cytokines that vary significantly in the absence of DUOX2 are represented in blue ( $n \geq 4$ ;  $p < 0.05$ ). Non-statistically significant variations are shown in gray. (C) Scatter plot of DUOX2-dependent cytokines and chemokine levels. DUOX2-independent cytokines and chemokines levels are shown in [Figure S2](#). Statistical comparisons were performed using a ratio-paired *t*-test with  $n \geq 4$  independent replicates. In (C), Geometric mean of ratios and significant *p*-value ( $< 0.05$ ) are indicated.

(CD63, CD35, CD66b), and interaction with immune complexes (CD16) status of neutrophils.<sup>46</sup> Neutrophils exposed to Ctrl-SeV Co-SN exhibited a significant increase of the surface mean expression of all five markers ([Figure 4F](#)). The absence of epithelial DUOX2 significantly impaired the capacity of Co-SN to induce surface mean expression of all markers but CD16 ([Figure 4F](#)). Results expressed in the percentage of positive cells follow the same trend although without reaching significance for most markers ([Figure S3](#)). This observation supports that adhesion and degranulation phenotypes of neutrophils induced by infection of ECs are DUOX2-dependent. Taken together, these results reveal previously unrecognized roles of DUOX2 in regulating soluble mediators secreted upon infection of ECs, which are important drivers of primary human neutrophil recruitment, adhesion, and degranulation.

### 3.4 | Epithelial DUOX2-dependent modulation of cytokines drives the activation and migratory phenotype of primary human neutrophils

Given the intriguing impact that epithelial DUOX2 displayed on neutrophil attraction and activation ([Figure 2](#)), we intended to further characterize this phenomenon. First, we tested whether replicating SeV in Co-SN contributed to the neutrophil phenotypes. Neutrophils were exposed to Ctrl-SeV Co-SN irradiated with UV to impair virions replication capacity.<sup>15</sup> No significant differences in neutrophil chemotaxis or surface marker expression were observed in response to UV-treated or untreated Ctrl-SeV Co-SN ([Figure 5A,B](#)), indicating that SeV replication is not responsible for changes observed in neutrophils phenotypes.

Several of the DUOX2-dependent cytokines/chemokines identified from the supernatants of SeV-infected A549 cells are classic neutrophil chemoattractants, including CXCL1, CXCL10, CCL7, CCL3, and TNF. The use of several chemokine receptor antagonists in chemotaxis assays showed that the blockade of CXCR2 using AZD5069 or CCR2/CCR5 by Cenicrivoc, but not CXCR3 using AMG487 or TNFR1 using R7050, significantly diminished

neutrophil directed movement ([Figure 6A](#)). Combined chemokine receptor antagonists had an additive effect on preventing neutrophil chemotaxis, by 38.5%, pointing to the concerted action of more than one receptor in driving neutrophil movement.

In the case of surface markers, blockade of TNFR1 diminished the expression of CD35, CD63, and CD11b induced by Ctrl-SeV Co-SN to a level similar to neutrophils exposed to Ctrl-Mock Co-SN, but not that of CD66b ([Figure 6B](#)). Finally, the combined antagonism of CXCR2, CXCR3, and CCR2/CCR5 selectively blocked the upregulation of CD11b ([Figure 6B](#)). Antagonism of G-CSF or GM-CSF did not reduce the expression of surface markers ([Figure 6B](#)) but rather resulted in an increased tendency. Altogether, these results demonstrate that SeV-infected ECs drive neutrophil migration and activation, in part through the DUOX2-dependent secretion of TNF and chemokines.

## 4 | DISCUSSION

Numerous studies have documented the key role of respiratory ECs in the early cytokine response and increasingly point to a major role in the recruitment and activation of different immune cell populations to the site of viral infection.<sup>36,47,48</sup> In line with this, we observed that A549 cells infected by SeV, used as a model of ssRNA virus, produce a mixture of soluble mediators, including cytokines and chemokines, that contribute to the activation of the innate host response through significant enhancement of neutrophils chemotaxis, NETosis, and expression of markers of adhesion and degranulation. The generation of DUOX2-deficient A549 cells using CRISPR-Cas9-mediated gene ablation enabled us to specifically address the role of DUOX2-dependent mechanisms in the response of ECs to virus infection. We first confirmed previous observations made by us and others using siRNA, that DUOX2 is essential for sustained levels of secreted IFN $\beta$ . Additionally, this model allowed us to highlight the selective role of DUOX2 in the control of the levels of a restricted panel of secreted cytokines and chemokines during the infection by SeV. The DUOX2-dependent secreted factors promote

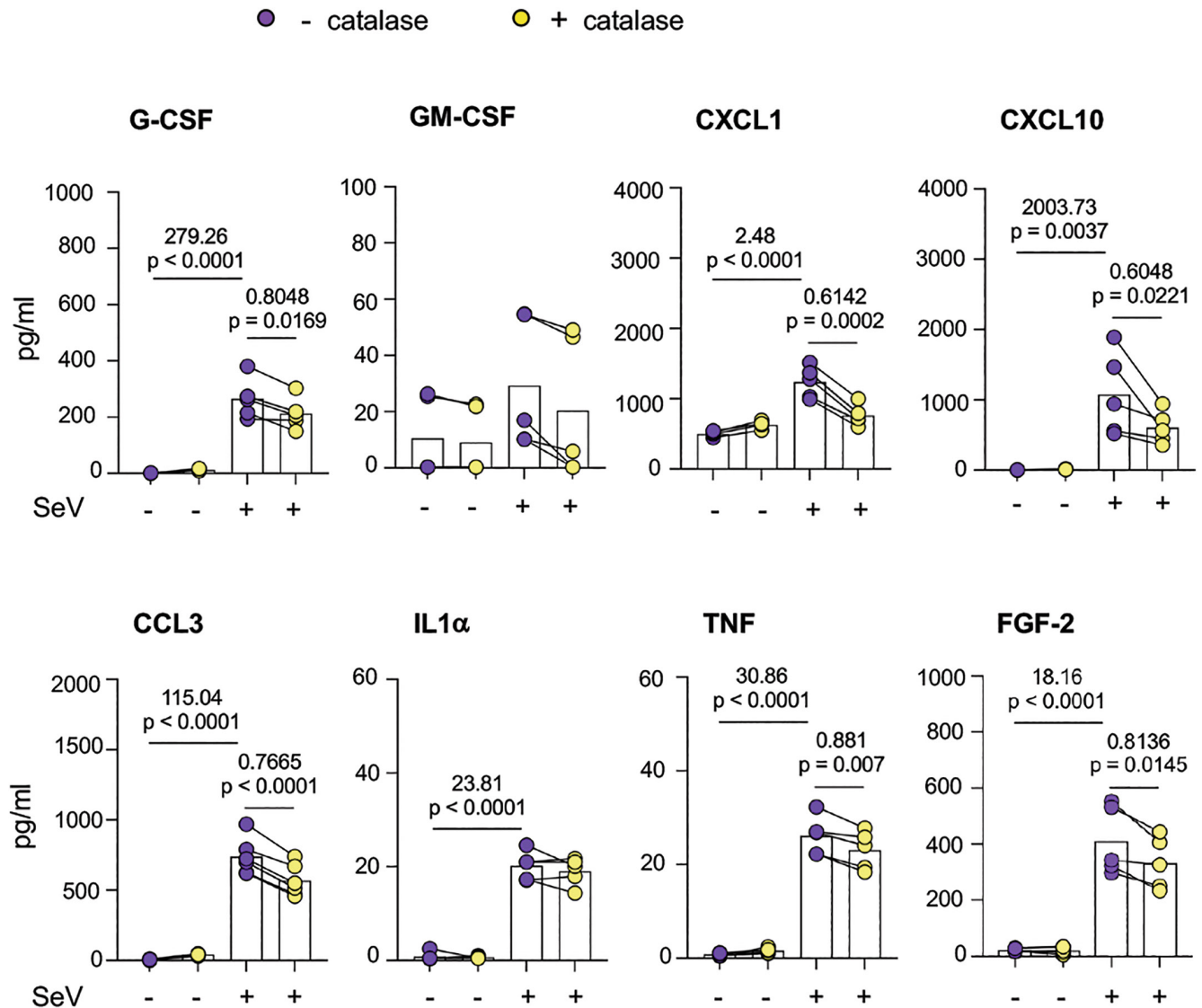


**FIGURE 3** Catalase reduces the cytokine response induced by SeV infection in epithelial cells. A549-Ctrl cells were left uninfected or infected with SeV (40 HAU/10<sup>6</sup> cells) for 24h in the absence (violet) or presence (yellow) of catalase (400 U/ml). Cytokines and chemokines release was quantified using Luminex-based multiplex assays. Statistical comparisons were performed using a ratio paired t-test with  $n \geq 5$  independent replicates. The geometric mean of ratios and significant  $p$ -value ( $< .05$ ) are indicated.

neutrophil chemotaxis, adhesion, and degranulation. In contrast, DUOX2 expression did not impact neutrophil viability or NETosis, thereby highlighting a selective impact of DUOX2 in neutrophil functions. Factors secreted by DUOX2-deficient ECs induced more neutrophil ROS production than those obtained from infected control cells. One might speculate that the absence of DUOX2 relieves negative feedback of ROS production by neutrophils. However, this response was extremely marginal, especially when compared to responses to classical agonists such as IgG aggregates, making physiological significance unlikely. Overall, this study unveils a new role of epithelial DUOX2 in early innate responses to virus infection.

The profile of the cytokines induced in our model of A549 cells infected with SeV, among which those whose

secreted levels were strongly dependent on DUOX2, namely G-CSF, GM-CSF, CXCL1, CXCL10, CCL3, CCL7, IL-1 $\alpha$ , FGF-2, and TNF, strongly overlaps with those observed in different models of ECs, including differentiated primary ECs, infected by viruses such as IAV and RSV.<sup>36,37</sup> The observation that epithelial DUOX2 controls the levels of a selected group of inflammatory cytokines and chemokines adds to our understanding of the role of DUOX2 in the immune response developed in response to RNA viruses. Previous data had documented the role of DUOX2 in the sustained production of type I and III IFNs following RSV and IAV infection.<sup>15,17</sup> In mouse models, induction of DUOX2 by rhinovirus (RV1B) and IAV protects against severe disease and lung pathology, in part through induction of the pathogen recognition receptors, RIG-I

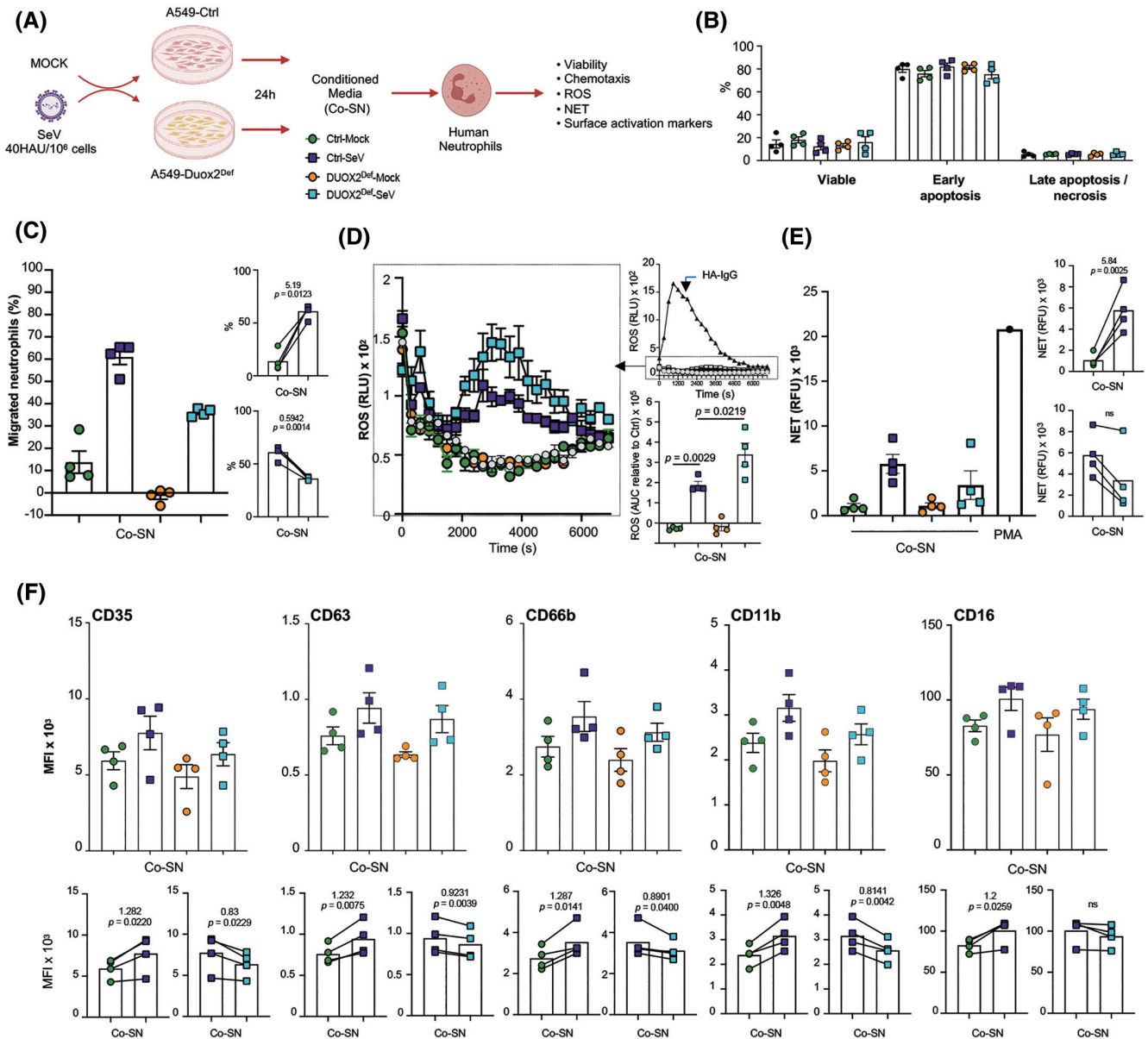


**FIGURE 4** DUOX2-dependent epithelial responses to SeV drive neutrophils migration, and expression of adhesion and degranulation surface markers. (A) Schematic representation of the experimental design. (B) Viability of neutrophils was assessed using Annexin V/PI staining. Data are shown as mean  $\pm$  SEM,  $n = 4$  independent experiments. (C) Neutrophils were allowed to migrate towards Co-SN in a chemotaxis system. Results are presented as percentages of migrated neutrophils and shown as mean  $\pm$  SEM of  $n = 4$  independent experiments. (D) Production of ROS by neutrophils was monitored using luminol for 120 min and expressed as relative light units (RLU). The top-right panel shows a representative experiment of the levels produced by neutrophils in response to heat aggregated (HA)-IgG or Co-SN (inside the dotted line rectangle). The latter are zoomed in the central panel. The bottom-right panel presents the mean  $\pm$  SEM of the corresponding areas under the curves (AUC) from  $n = 4$  independent experiments. (E) NET production was assessed using SYTOX green and expressed as relative fluorescence units (RFU). PMA stimulation was used as a positive control. The mean  $\pm$  SEM of  $n = 4$  independent experiments are shown. (F) Selected surface marker expression was measured by flow cytometry. Mean  $\pm$  SEM of mean fluorescence intensities (MFI) from  $n = 4$  independent experiments are shown. Statistical comparisons were performed using a ratio paired t-test. The geometric mean of ratios and  $p$ -value are indicated. Co-SN: Conditioned supernatant. Ctrl-Mock (green circle): A549-Ctrl, uninfected; Ctrl-SeV (violet square): A549-Ctrl, infected SeV; DUOX2<sup>Def</sup>-Mock (orange circle): A549-DUOX2<sup>Def</sup>, uninfected; DUOX2<sup>Def</sup>-SeV (blue square): A549-DUOX2<sup>Def</sup>, infected with SeV.

and MDA5.<sup>17,21,24</sup> Our finding that DUOX2 controls only a selective number of cytokines and chemokines among those induced by SeV was intriguing. Interestingly, in a mouse model, epithelial DUOX1 was also shown to shape

the early cytokine response to IAV in the lung through the upregulation of CCL27, IL-1 $\beta$ , and CXCL5 and to a lesser extent IL-2, CCL1, CCL3, CCL11, CCL19, CCL20, and CXCL1.<sup>18</sup> It is noteworthy that there is minimal

Co-SN: ● Ctrl-Mock ■ Ctrl-SeV ▼ Ctrl-SeV + UV

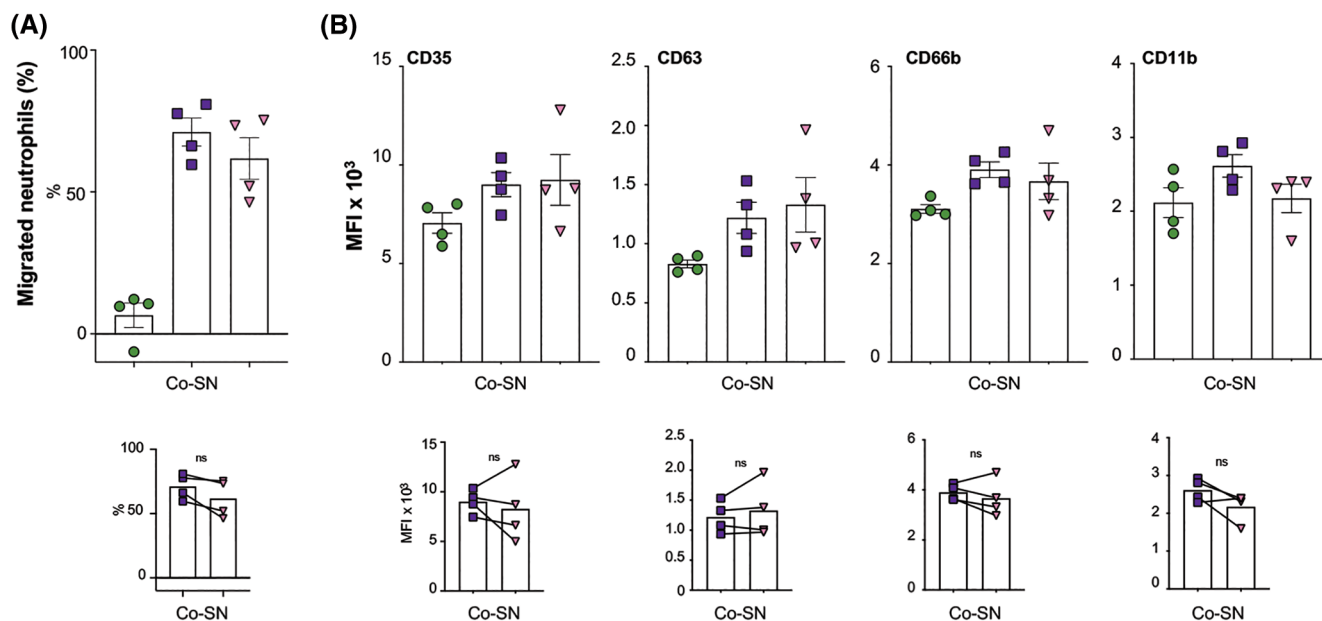


**FIGURE 5** Replicating SeV is not responsible for changes observed in neutrophil phenotypes. Neutrophils were treated with epithelial cell-derived conditioned media (Co-SN) pre-treated or not with UV. (A) Neutrophil migration quantified using a chemotaxis system is expressed as % of migrated neutrophils. The mean  $\pm$  SEM of  $n = 4$  independent experiments is shown. (B) Expression of DUOX2-dependent surface markers (as determined in Figure 4) was monitored by flow cytometry. The mean  $\pm$  SEM of the mean fluorescence intensities is shown ( $n = 4$  independent experiments). Statistical comparisons were performed using a ratio-paired t-test. The geometric mean of ratios and  $p$ -value are indicated. Co-SN used: Ctrl-Mock (green circle); Ctrl-SeV (violet square); Ctrl-SeV treated with UV (pink triangle).

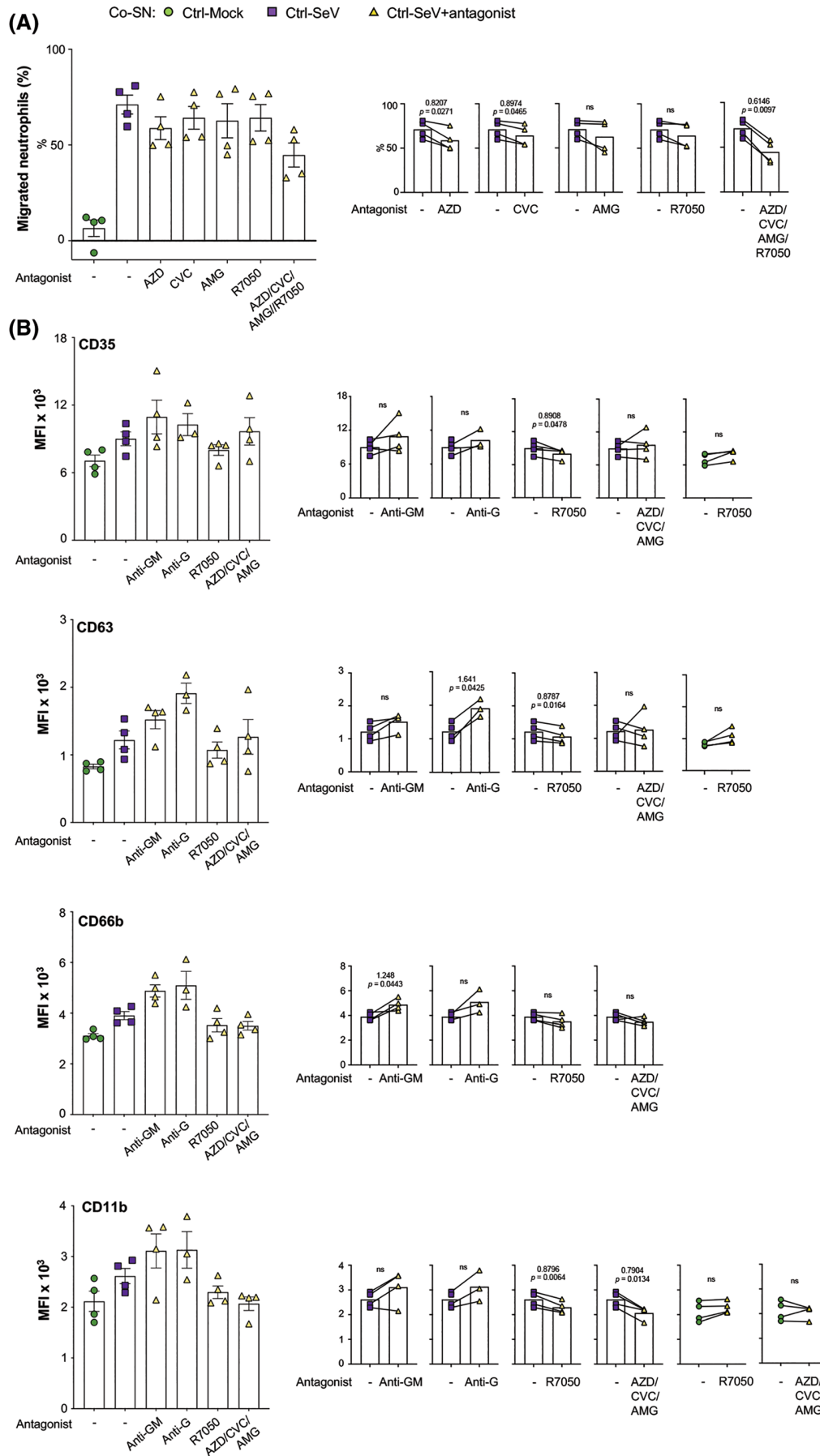
overlapping in the cytokines and chemokines found regulated by DUOX1 and the ones regulated by DUOX2 identified in this study. This argues toward a model in which both DUOX have non-redundant roles in the regulation of chemokine and cytokine response following respiratory viral infections. This prompts future studies to address this hypothesis and determine the underlying mechanism, which may rely on distinct localization or expression levels throughout the kinetics of viral infection.

Oxidative stress induced by  $O_3$  has been reported to trigger neutrophil lung recruitment through the transcriptional regulation *CCL7* and *CXCL10* in BALB/C mice model.<sup>44</sup> Similarly, we previously observed a NOX2-dependent transcriptional regulation of antiviral genes in ECs infected with SeV and RSV.<sup>14</sup> In this study, the NF- $\kappa$ B, IRF-3, and Jak/STAT inflammatory signaling pathways

known to control the transcription of induced immunoregulatory genes in response to RNA viruses in the airway epithelium were not affected by the absence of DUOX2. This observation is consistent with our previous report that DUOX2 silencing in A549 cells and primary NHBE did not alter the induction of IFN $\beta$ , IFN $\lambda$ , or TNF mRNAs by SeV, while decreasing their secreted levels.<sup>15</sup> This indicates a DUOX2-dependent regulatory mechanism that does not involve key immune signaling pathways. A possible alternative mechanism could be the regulation of cytokine trafficking. Indeed, a recent study in human macrophages subjected to substance P highlighted the role of DUOX2 in the production of the soluble extracellular form of CX3CL1 via the  $H_2O_2$ -dependent activation of the metalloprotease activity of ADAM10/17.<sup>49</sup> Similarly, DUOX1-mediated oxidative activation of Src kinase and

**FIGURE 6** DUOX2-dependent cytokines secreted by SeV-infected ECs drive neutrophil migratory and activation phenotype. Neutrophils were pre-treated with 2  $\mu$ M TNF receptor-I antagonist R7050, 100 nM CXCR2 antagonist AZD5069 (AZD), 1  $\mu$ M CXCR3 antagonist AMG487 (AMG), 1  $\mu$ M CCR2-CCR5 antagonist Cenicrivoc (CVC), alone or in combination as indicated before stimulation with conditioned supernatant (Co-SN). Alternatively, neutrophils were exposed to Co-SN preincubated with 10  $\mu$ g/ml anti-GM-CSF (anti-GM) or anti-G-CSF (anti-G) neutralizing antibodies. (A) Percentages of migrated neutrophils in a chemotaxis system are shown as mean  $\pm$  SEM of  $n = 4$  independent experiments. (B) Expression of DUOX2-dependent surface markers was quantified by flow cytometry. Mean fluorescence intensities are shown as the mean  $\pm$  SEM of  $n = 4$  independent experiments. Statistical comparisons were performed using a ratio-paired t-test. The geometric mean of ratios and  $p$ -value are indicated. Co-SN used: Ctrl-Mock (green circle); Ctrl-SeV (violet square); Ctrl-SeV + the indicated antagonist (yellow triangle).





EGFR was shown to be critical for calpain-2-dependent IL-33 secretion in airway ECs challenged with allergens.<sup>50</sup> Further studies will be required to elucidate the molecular mechanisms involved in DUOX2-dependent regulation of selected cytokines and chemokines in virus-infected ECs.

Timely neutrophil attraction to the site of infection results from the complex and coordinated action of multiple chemoattractive factors.<sup>51,52</sup> Our data suggest an additive effect of CXCR2- and CCR2/CCR5-ligands present in ECs-derived Co-SN. Among chemokines that bind to these receptors that were induced in ECs upon SeV infection, CXCL1, CCL7, and CCL3 were dependent on DUOX2, but not CXCL8, CCL2, CCL4, CCL5, or CCL8. This is consistent with the observation that the absence of DUOX2 in ECs only partially impaired neutrophil chemotaxis. This points towards a complex regulation of neutrophil migration by a combination of DUOX2-dependent and DUOX2-independent factors secreted by ECs. Although chemokines are clearly important for the recruitment of neutrophils, H<sub>2</sub>O<sub>2</sub> is also a potent neutrophil chemoattractant.<sup>53,54</sup> Notably, DUOX-derived H<sub>2</sub>O<sub>2</sub> was shown to form a concentration gradient, guiding neutrophil toward the wound in zebrafish and drosophila models.<sup>55–58</sup> Although this function remains to be demonstrated in the mammalian respiratory tract, one might speculate that DUOX2 could contribute to neutrophils' attraction to infected ECs, both through the regulation of chemokines and H<sub>2</sub>O<sub>2</sub>.

In addition to chemotaxis, EC-secreted DUOX2-dependent factors were also found to upregulate neutrophil adhesion and degranulation markers, suggesting that epithelial DUOX2 is also important for the activation of infiltrated neutrophils. Among the cytokines and chemokines secreted in a DUOX2-dependent manner, TNF appears to be key for the induction of both CD11b adhesion marker and exocytosis of secretory vesicles and azurophilic granules as assessed by CD35 and CD63 surface expression, while chemokine binding to CXCR2 and/or CCR2/CCR5 receptors have a limited impact and act only on the induction of the adhesion marker CD11b. Of note, G-CSF and GM-CSF, which ranked among the most negatively affected secreted factors in DUOX2-deficient ECs infected by SeV, were not found to be major contributors to the surface expression of any of the adhesion and degranulation markers.

Neutrophils, the most abundant circulating innate immune cells, are present in healthy lungs in low numbers but rapidly accumulate as a result of respiratory virus infection.<sup>59–62</sup> They concentrate at specific foci coincident with virus-positive epithelium<sup>63–66</sup> where they contribute to the control of virus infections through diverse effector functions, namely phagocytosis,<sup>64,67</sup> oxidative burst,<sup>68</sup> exocytosis of secretory vesicles and azurophilic and specific granules that increase responses to PAMPs and release

myeloperoxidase and proteases<sup>69–73</sup> and NETosis.<sup>74–76</sup> Although beneficial for antiviral immunity, inappropriate and/or prolonged neutrophil activation is thought to be implicated in adverse host effects. This is consistent with observations that neutrophilia is positively correlated with disease severity associated with several respiratory viral infections, including IAV-induced ARDS, bronchiolitis associated with RSV infection, and COVID-19 caused by SARS-CoV-2.<sup>77–82</sup> Notably, neutrophils have been implicated in tissue damage and epithelial integrity disruption, as well as obstruction of the airway and limitation of gas exchange during severe respiratory viral infections.<sup>39,66,82–85</sup> This paradox pinpoints the importance of a finely tuned neutrophilic response for achieving effective immune protection while avoiding detrimental damage.<sup>86</sup>

Our results reveal previously unrecognized roles of epithelial DUOX2 in the regulation of soluble mediators secreted during EC infection. Our findings also highlight the importance of this role of DUOX2 as a decisive host factor contributing to the recruitment, adhesion, and degranulation of neutrophils in respiratory infections. This novel role of DUOX2 in the epithelial-neutrophil cross-talk opens future avenues of research toward a better understanding of the mechanisms that determine the degree and quality of neutrophil response in the lung during respiratory virus infection. This could guide future interventions aimed at preventing events that may lead to unbridled inflammation responsible for severe disease.

## AUTHOR CONTRIBUTIONS

Nathalie Grandvaux conceived and designed the research. Dacquin M. Kasumba, Marc Pouliot, and Nathalie Grandvaux designed the experiments and analyzed and interpreted the data. Dacquin M. Kasumba, Sandrine Huot, Elise Caron, Audray Fortin, Cynthia Laflamme, Natalia Zamorano Cuervo and Felix Lamontagne performed the experiments. Dacquin M. Kasumba, Felix Lamontagne, Marc Pouliot, and Nathalie Grandvaux were involved in drafting and revising the manuscript. All authors approved the final version of the manuscript.

## ACKNOWLEDGMENTS

The present work was funded by grants from the Canadian Institutes of Health Research (CIHR) [MOP-137099 and III-134054] to NG and by a research grant “Initiatives de la pandémie de COVID19” from the Fonds de recherche du Québec – Santé (FRQS) [295847] to NG and MP. DK was a recipient of a postdoctoral fellowship from Réseau de Recherche en Santé Respiratoire du Québec (RSRQ). SH is the recipient of a Frederick Banting & Charles Best studentship from the Canadian Institutes of Health Research (CIHR). NZC was a recipient of graduate studentships from the Faculty of Medicine, the Faculty

of post-doctoral and graduate studies, Université de Montréal, and FRQS. NZC, FL, and NG are members of the RSRQ. NZC, FL, MP, and NG are members of the Réseau Québécois COVID – Pandémie (RQCP).

## DISCLOSURES

The authors declare that they have no competing interests.

## DATA AVAILABILITY STATEMENT

Data sharing is not applicable to this article as no datasets were generated or analyzed during the current study.

## ORCID

Marc Pouliot  <https://orcid.org/0000-0002-2466-5424>

Nathalie Grandvaux  <https://orcid.org/0000-0003-0567-0284>

## REFERENCES

- Rao S, Nyquist AC. Respiratory viruses and their impact in healthcare. *Curr Opin Infect Dis.* 2014;27(4):342-347. doi:10.1097/qco.0000000000000079
- Smith Jervelund S, Eikemo TA. The double burden of COVID-19. *Scand J Public Health.* 2021;49(1):1-4. doi:10.1177/1403494820984702
- Boncristiani HF, Criado MF, Arruda E. Respiratory viruses. *Encyclopedia of Microbiology.* Elsevier; 2009:500-518. doi:10.1016/b978-012373944-5.00314-x
- Camp JV, Jonsson CB. A role for neutrophils in viral respiratory disease. *Front Immunol.* 2017;8:550. doi:10.3389/fimmu.2017.00550
- Mettelman RC, Allen EK, Thomas PG. Mucosal immune responses to infection and vaccination in the respiratory tract. *Immunity.* 2022;55(5):749-780. doi:10.1016/j.immuni.2022.04.013
- Miura TA. Respiratory epithelial cells as master communicators during viral infections. *Curr Clin Microbiol Rep.* 2019;6(1):10-17. doi:10.1007/s40588-019-0111-8
- Kikkert M. Innate immune evasion by human respiratory RNA viruses. *J Innate Immun.* 2020;12(1):4-20. doi:10.1159/000503030
- Ouyang Y, Liao H, Hu Y, Luo K, Hu S, Zhu H. Innate immune evasion by human respiratory syncytial virus. *Front Microbiol.* 2022;13:865592. doi:10.3389/fmicb.2022.865592
- Rosenberg HF, Domachowske JB. Inflammatory responses to respiratory syncytial virus (RSV) infection and the development of immunomodulatory pharmacotherapeutics. *Curr Med Chem.* 2012;19(10):1424-1431. doi:10.2174/092986712799828346
- Li Z, Xu X, Leng X, et al. Roles of reactive oxygen species in cell signaling pathways and immune responses to viral infections. *Arch Virol.* 2017;162(3):603-610. doi:10.1007/s00705-016-3130-2
- Sander WJ, Fourie C, Sabiu S, O'Neill FH, Pohl CH, O'Neill HG. Reactive oxygen species as potential antiviral targets. *Rev Med Virol.* 2022;32(1):e2240. doi:10.1002/rmv.2240
- Khomich OA, Kochetkov SN, Bartosch B, Ivanov AV. Redox biology of respiratory viral infections. *Viruses.* 2018;10(8):392. doi:10.3390/v10080392
- Grandvaux N, Mariani M, Fink K. Lung epithelial NOX/DUOX and respiratory virus infections. *Clin Sci.* 2015;128(6):337-347. doi:10.1042/cs20140321
- Fink K, Duval A, Martel A, Soucy-Faulkner A, Grandvaux N. Dual role of NOX2 in respiratory syncytial virus- and Sendai virus-induced activation of NF-kappaB in airway epithelial cells. *J Immunol.* 2008;180(10):6911-6922. doi:10.4049/jimmunol.180.10.6911
- Fink K, Martin L, Mukawera E, et al. IFNbeta/TNFalpha synergism induces a non-canonical STAT2/IRF9-dependent pathway triggering a novel DUOX2 NADPH oxidase-mediated airway antiviral response. *Cell Res.* 2013;23(5):673-690. doi:10.1038/cr.2013.47
- Kim HJ, Kim CH, Ryu JH, et al. Reactive oxygen species induce antiviral innate immune response through IFN-lambda regulation in human nasal epithelial cells. *Am J Respir Cell Mol Biol.* 2013;49(5):855-865. doi:10.1165/rcmb.2013-0003OC
- Strengert M, Jennings R, Davanture S, Hayes P, Gabriel G, Knaus UG. Mucosal reactive oxygen species are required for antiviral response: role of Duox in influenza a virus infection. *Antioxid Redox Signal.* 2013;20(17):2695-2709. doi:10.1089/ars.2013.5353
- Sarr D, Gingerich AD, Asthiwi NM, et al. Dual oxidase 1 promotes antiviral innate immunity. *Proc Natl Acad Sci U S A.* 2021;118(26):e2017130118. doi:10.1073/pnas.2017130118
- Kim HJ, Kim CH, Kim MJ, et al. The induction of pattern-recognition receptor expression against influenza a virus through Duox2-derived reactive oxygen species in nasal mucosa. *Am J Respir Cell Mol Biol.* 2015;53(4):525-535. doi:10.1165/rcmb.2014-0334OC
- Comstock AT, Ganesan S, Chatteraj A, et al. Rhinovirus-induced barrier dysfunction in polarized airway epithelial cells is mediated by NADPH oxidase 1. *J Virol.* 2011;85(13):6795-6808. doi:10.1128/JVI.02074-10
- Harper RW, Xu C, Eiserich JP, et al. Differential regulation of dual NADPH oxidases/peroxidases, Duox1 and Duox2, by Th1 and Th2 cytokines in respiratory tract epithelium. *FEBS Lett.* 2005;579(21):4911-4917. doi:10.1016/j.febslet.2005.08.002
- Moolamalla STR, Balasubramanian R, Chauhan R, Priyakumar UD, Vinod PK. Host metabolic reprogramming in response to SARS-CoV-2 infection: a systems biology approach. *Microb Pathog.* 2021;158:105114. doi:10.1016/j.micpath.2021.105114
- Kim HJ, Seo YH, An S, Jo A, Kwon IC, Kim S. Chemiluminescence imaging of Duox2-derived hydrogen peroxide for longitudinal visualization of biological response to viral infection in nasal mucosa. *Theranostics.* 2018;8(7):1798-1807. doi:10.7150/thno.22481
- Hong SN, Kim JY, Kim H, et al. Duox2 is required for the transcription of pattern recognition receptors in acute viral lung infection: An interferon-independent regulatory mechanism. *Antiviral Res.* 2016;134:1-5. doi:10.1016/j.antiviral.2016.08.017
- Kim BJ, Cho SW, Jeon YJ, et al. Intranasal delivery of Duox2 DNA using cationic polymer can prevent acute influenza a viral infection in vivo lung. *Appl Microbiol Biotechnol.* 2018;102(1):105-115. doi:10.1007/s00253-017-8512-1
- Robitaille AC, Mariani MK, Fortin A, Grandvaux N. A high resolution method to monitor phosphorylation-dependent activation of IRF3. *J Vis Exp.* 2016;(107):e53723. doi:10.3791/53723
- Servant MJ, Grandvaux N, tenOever BR, Duguay D, Lin R, Hiscott J. Identification of the minimal phosphoacceptor site required for in vivo activation of interferon regulatory factor 3 in response to virus and double-stranded RNA. *J Biol Chem.* 2003;278(11):9441-9447. doi:10.1074/jbc.M209851200

28. Fiset ME, Gilbert C, Poubelle PE, Pouliot M. Human neutrophils as a source of nociceptin: a novel link between pain and inflammation. *Biochemistry*. 2003;42(35):10498-10505. doi:10.1021/bi0300635
29. Frevert CW, Wong VA, Goodman RB, Goodwin R, Martin TR. Rapid fluorescence-based measurement of neutrophil migration in vitro. *J Immunol Methods*. 1998;213(1):41-52. doi:10.1016/s0022-1759(98)00016-7
30. McColl SR, St-Onge M, Dussault AA, et al. Immunomodulatory impact of the A2A adenosine receptor on the profile of chemokines produced by neutrophils. *FASEB J*. 2006;20(1):187-189. doi:10.1096/fj.05-4804fje
31. Fossati G, Bucknall RC, Edwards SW. Insoluble and soluble immune complexes activate neutrophils by distinct activation mechanisms: changes in functional responses induced by priming with cytokines. *Ann Rheum Dis*. 2002;61(1):13-19. doi:10.1136/ard.61.1.13
32. Gray RD, Lucas CD, MacKellar A, et al. Activation of conventional protein kinase C (PKC) is critical in the generation of human neutrophil extracellular traps. *J Inflamm*. 2013;10(1):12. doi:10.1186/1476-9255-10-12
33. Yoneyama M, Onomoto K, Jogi M, Akaboshi T, Fujita T. Viral RNA detection by RIG-I-like receptors. *Curr Opin Immunol*. 2015;32:48-53. doi:10.1016/j.coi.2014.12.012
34. Platanias LC. Mechanisms of type-I- and type-II-interferon-mediated signalling. *Nat Rev Immunol*. 2005;5(5):375-386. doi:10.1038/nri1604
35. Vallabhapurapu S, Karin M. Regulation and function of NF-kappaB transcription factors in the immune system. *Annu Rev Immunol*. 2009;27:693-733. doi:10.1146/annurev.immunol.021908.132641
36. Glaser L, Coulter PJ, Shields M, Touzelet O, Power UF, Broadbent L. Airway epithelial derived cytokines and chemokines and their role in the immune response to respiratory syncytial virus infection. *Pathogens*. 2019;8(3):106. doi:10.3390/pathogens8030106
37. Ioannidis I, McNally B, Willette M, et al. Plasticity and virus specificity of the airway epithelial cell immune response during respiratory virus infection. *J Virol*. 2012;86(10):5422-5436. doi:10.1128/JVI.06757-11
38. Parkos CA. Neutrophil-epithelial interactions: a double-edged sword. *Am J Pathol*. 2016;186(6):1404-1416. doi:10.1016/j.ajpath.2016.02.001
39. Deng Y, Herbert JA, Robinson E, Ren L, Smyth RL, Smith CM. Neutrophil-airway epithelial interactions result in increased epithelial damage and viral clearance during respiratory syncytial virus infection. *J Virol*. 2020;94(13):e02161-19. doi:10.1128/JVI.02161-19
40. Bendall LJ, Bradstock KF. G-CSF: from granulopoietic stimulant to bone marrow stem cell mobilizing agent. *Cytokine Growth Factor Rev*. 2014;25(4):355-367. doi:10.1016/j.cytogfr.2014.07.011
41. Castellani S, D'Oria S, Diana A, et al. G-CSF and GM-CSF modify neutrophil functions at concentrations found in cystic fibrosis. *Sci Rep*. 2019;9(1):12937. doi:10.1038/s41598-019-49419-z
42. Smart SJ, Casale TB. Pulmonary epithelial cells facilitate TNF-alpha-induced neutrophil chemotaxis. A role for cytokine networking. *J Immunol*. 1994;152(8):4087-4094.
43. Bonville CA, Percopo CM, Dyer KD, et al. Interferon-gamma coordinates CCL3-mediated neutrophil recruitment in vivo. *BMC Immunol*. 2009;10:14. doi:10.1186/1471-2172-10-14
44. Michalec L, Choudhury BK, Postlethwait E, et al. CCL7 and CXCL10 orchestrate oxidative stress-induced neutrophilic lung inflammation. *J Immunol*. 2002;168(2):846-852. doi:10.4049/jimmunol.168.2.846
45. Gale R, Bertouch JV, Gordon TP, Bradley J, Roberts-Thomson PJ. Neutrophil activation by immune complexes and the role of rheumatoid factor. *Ann Rheum Dis*. 1984;43(1):34-39. doi:10.1136/ard.43.1.34
46. Huot S, Laflamme C, Fortin PR, Boilard E, Pouliot M. IgG-aggregates rapidly upregulate FcγRI expression at the surface of human neutrophils in a FcγRII-dependent fashion: a crucial role for FcγRI in the generation of reactive oxygen species. *FASEB J*. 2020;34(11):15208-15221. doi:10.1096/fj.202001085R
47. Chua RL, Lukassen S, Trump S, et al. COVID-19 severity correlates with airway epithelium-immune cell interactions identified by single-cell analysis. *Nat Biotechnol*. 2020;38(8):970-979. doi:10.1038/s41587-020-0602-4
48. Thorne LG, Reuschl AK, Zuliani-Alvarez L, et al. SARS-CoV-2 sensing by RIG-I and MDA5 links epithelial infection to macrophage inflammation. *EMBO J*. 2021;40(15):e107826. doi:10.15252/emboj.2021107826
49. Yamaguchi R, Haraguchi M, Yamaguchi R, et al. TRIM28/TIF1β and Fli-1 negatively regulate peroxynitrite generation via DUOX2 to decrease the shedding of membrane-bound fractalkine in human macrophages after exposure to substance P. *Cytokine*. 2020;134:155180. doi:10.1016/j.cyto.2020.155180
50. Hristova M, Habibovic A, Veith C, et al. Airway epithelial dual oxidase 1 mediates allergen-induced IL-33 secretion and activation of type 2 immune responses. *J Allergy Clin Immunol*. 2016;137(5):1545-1556.e11. doi:10.1016/j.jaci.2015.10.003
51. Metzemaekers M, Gouwy M, Proost P. Neutrophil chemoattractant receptors in health and disease: double-edged swords. *Cell Mol Immunol*. 2020;17(5):433-450. doi:10.1038/s41423-020-0412-0
52. Rajarathnam K, Schnoor M, Richardson RM, Rajagopal S. How do chemokines navigate neutrophils to the target site: dissecting the structural mechanisms and signaling pathways. *Cell Signal*. 2019;54:69-80. doi:10.1016/j.cellsig.2018.11.004
53. Klyubin IV, Kirpichnikova KM, Gamaley IA. Hydrogen peroxide-induced chemotaxis of mouse peritoneal neutrophils. *Eur J Cell Biol*. 1996;70(4):347-351.
54. Morad H, Luqman S, Tan CH, Swann V, McNaughton PA. TRPM2 ion channels steer neutrophils towards a source of hydrogen peroxide. *Sci Rep*. 2021;11(1):9339. doi:10.1038/s41598-021-88224-5
55. Niethammer P, Grabher C, Look AT, Mitchison TJ. A tissue-scale gradient of hydrogen peroxide mediates rapid wound detection in zebrafish. *Nature*. 2009;459(7249):996-999. doi:10.1038/nature08119
56. Razzell W, Evans IR, Martin P, Wood W. Calcium flashes orchestrate the wound inflammatory response through DUOX activation and hydrogen peroxide release. *Curr Biol*. 2013;23(5):424-429. doi:10.1016/j.cub.2013.01.058
57. Yoo SK, Starnes TW, Deng Q, Huttenlocher A. Lyn is a redox sensor that mediates leukocyte wound attraction in vivo. *Nature*. 2011;480(7375):109-112. doi:10.1038/nature10632
58. Bernut A, Loynes CA, Floto RA, Renshaw SA. Deletion of cfr leads to an excessive neutrophilic response and defective tissue repair in a zebrafish model of sterile inflammation. *Front Immunol*. 2020;11:1733. doi:10.3389/fimmu.2020.01733



59. Watanabe T, Tisoncik-Go J, Tchitchek N, et al. 1918 influenza virus hemagglutinin (HA) and the viral RNA polymerase complex enhance viral pathogenicity, but only HA induces aberrant host responses in mice. *J Virol.* 2013;87(9):5239-5254. doi:[10.1128/JVI.02753-12](https://doi.org/10.1128/JVI.02753-12)
60. Long JP, Kotur MS, Stark GV, et al. Accumulation of CD11b(+) gr-1(+) cells in the lung, blood and bone marrow of mice infected with highly pathogenic H5N1 and H1N1 influenza viruses. *Arch Virol.* 2013;158(6):1305-1322. doi:[10.1007/s00705-012-1593-3](https://doi.org/10.1007/s00705-012-1593-3)
61. Zhu H, Wang D, Kelvin DJ, et al. Infectivity, transmission, and pathology of human-isolated H7N9 influenza virus in ferrets and pigs. *Science.* 2013;341(6142):183-186. doi:[10.1126/science.1239844](https://doi.org/10.1126/science.1239844)
62. Geerdink RJ, Pillay J, Meyaard L, Bont L. Neutrophils in respiratory syncytial virus infection: a target for asthma prevention. *J Allergy Clin Immunol.* 2015;136(4):838-847. doi:[10.1016/j.jaci.2015.06.034](https://doi.org/10.1016/j.jaci.2015.06.034)
63. Camp JV, Bagci U, Chu YK, et al. Lower respiratory tract infection of the ferret by 2009 H1N1 pandemic influenza a virus triggers biphasic, systemic, and local recruitment of neutrophils. *J Virol.* 2015;89(17):8733-8748. doi:[10.1128/JVI.00817-15](https://doi.org/10.1128/JVI.00817-15)
64. Ratcliffe D, Migliorisi G, Cramer E. Translocation of influenza virus by migrating neutrophils. *Cell Mol Biol.* 1992;38(1):63-70.
65. Ratcliffe DR, Nolin SL, Cramer EB. Neutrophil interaction with influenza-infected epithelial cells. *Blood.* 1988;72(1):142-149.
66. Wang SZ, Xu H, Wraith A, Bowden JJ, Alpers JH, Forsyth KD. Neutrophils induce damage to respiratory epithelial cells infected with respiratory syncytial virus. *Eur Respir J.* 1998;12(3):612-618.
67. LeVine AM, Elliott J, Whitsett JA, et al. Surfactant protein-d enhances phagocytosis and pulmonary clearance of respiratory syncytial virus. *Am J Respir Cell Mol Biol.* 2004;31(2):193-199. doi:[10.1165/rcmb.2003-0107OC](https://doi.org/10.1165/rcmb.2003-0107OC)
68. Saitoh T, Komano J, Saitoh Y, et al. Neutrophil extracellular traps mediate a host defense response to human immunodeficiency virus-1. *Cell Host Microbe.* 2012;12(1):109-116. doi:[10.1016/j.chom.2012.05.015](https://doi.org/10.1016/j.chom.2012.05.015)
69. Doss M, White MR, Teclé T, et al. Interactions of alpha-, beta-, and theta-defensins with influenza a virus and surfactant protein D. *J Immunol.* 2009;182(12):7878-7887. doi:[10.4049/jimmunol.0804049](https://doi.org/10.4049/jimmunol.0804049)
70. Teclé T, White MR, Gantz D, Crouch EC, Hartshorn KL. Human neutrophil defensins increase neutrophil uptake of influenza a virus and bacteria and modify virus-induced respiratory burst responses. *J Immunol.* 2007;178(12):8046-8052. doi:[10.4049/jimmunol.178.12.8046](https://doi.org/10.4049/jimmunol.178.12.8046)
71. Yamamoto K, Miyoshi-Koshio T, Utsuki Y, Mizuno S, Suzuki K. Virucidal activity and viral protein modification by myeloperoxidase: a candidate for defense factor of human polymorphonuclear leukocytes against influenza virus infection. *J Infect Dis.* 1991;164(1):8-14. doi:[10.1093/infdis/164.1.8](https://doi.org/10.1093/infdis/164.1.8)
72. Borregaard N, Sorensen OE, Theilgaard-Monch K. Neutrophil granules: a library of innate immunity proteins. *Trends Immunol.* 2007;28(8):340-345. doi:[10.1016/j.it.2007.06.002](https://doi.org/10.1016/j.it.2007.06.002)
73. Bradley LM, Douglass MF, Chatterjee D, Akira S, Baaten BJ. Matrix metalloprotease 9 mediates neutrophil migration into the airways in response to influenza virus-induced toll-like receptor signaling. *PLoS Pathog.* 2012;8(4):e1002641. doi:[10.1371/journal.ppat.1002641](https://doi.org/10.1371/journal.ppat.1002641)
74. Galani IE, Andreakos E. Neutrophils in viral infections: current concepts and caveats. *J Leukoc Biol.* 2015;98(4):557-564. doi:[10.1189/jlb.4VMR1114-555R](https://doi.org/10.1189/jlb.4VMR1114-555R)
75. Schonrich G, Raftery MJ. Neutrophil extracellular traps go viral. *Front Immunol.* 2016;7:366. doi:[10.3389/fimmu.2016.00366](https://doi.org/10.3389/fimmu.2016.00366)
76. Raftery MJ, Lalwani P, Krautkrmer E, et al. beta2 integrin mediates hantavirus-induced release of neutrophil extracellular traps. *J Exp Med.* 2014;211(7):1485-1497. doi:[10.1084/jem.20131092](https://doi.org/10.1084/jem.20131092)
77. Prozan L, Shusterman E, Ablin J, et al. Prognostic value of neutrophil-to-lymphocyte ratio in COVID-19 compared with influenza and respiratory syncytial virus infection. *Sci Rep.* 2021;11(1):21519. doi:[10.1038/s41598-021-00927-x](https://doi.org/10.1038/s41598-021-00927-x)
78. George ST, Lai J, Ma J, Stacey HD, Miller MS, Mullarkey CE. Neutrophils and influenza: a thin line between helpful and harmful. *Vaccine.* 2021;9(6):597. doi:[10.3390/vaccines9060597](https://doi.org/10.3390/vaccines9060597)
79. Weiland JE, Davis WB, Holter JF, Mohammed JR, Dorinsky PM, Gadek JE. Lung neutrophils in the adult respiratory distress syndrome. Clinical and pathophysiologic significance. *Am Rev Respir Dis.* 1986;133(2):218-225. doi:[10.1164/arrd.1986.133.2.218](https://doi.org/10.1164/arrd.1986.133.2.218)
80. McNamara PS, Ritson P, Selby A, Hart CA, Smyth RL. Bronchoalveolar lavage cellularity in infants with severe respiratory syncytial virus bronchiolitis. *Arch Dis Child.* 2003;88(10):922-926. doi:[10.1136/adc.88.10.922](https://doi.org/10.1136/adc.88.10.922)
81. Xia X, Wen M, Zhan S, He J, Chen W. An increased neutrophil/lymphocyte ratio is an early warning signal of severe COVID-19. *Nan Fang Yi Ke Da Xue Xue Bao.* 2020;40(3):333-336. doi:[10.12122/j.issn.1673-4254.2020.03.06](https://doi.org/10.12122/j.issn.1673-4254.2020.03.06)
82. Haick AK, Rzepka JP, Brandon E, Balemba OB, Miura TA. Neutrophils are needed for an effective immune response against pulmonary rat coronavirus infection, but also contribute to pathology. *J Gen Virol.* 2014;95(Pt 3):578-590. doi:[10.1099/vir.0.061986-0](https://doi.org/10.1099/vir.0.061986-0)
83. Sorensen OE, Borregaard N. Neutrophil extracellular traps - the dark side of neutrophils. *J Clin Invest.* 2016;126(5):1612-1620. doi:[10.1172/JCI84538](https://doi.org/10.1172/JCI84538)
84. Yang SC, Tsai YF, Pan YL, Hwang TL. Understanding the role of neutrophils in acute respiratory distress syndrome. *Biom J.* 2020;44(4):439-446. doi:[10.1016/j.bj.2020.09.001](https://doi.org/10.1016/j.bj.2020.09.001)
85. Thierry AR, Roch B. Neutrophil extracellular traps and by-products play a key role in COVID-19: pathogenesis, risk factors, and therapy. *J Clin Med.* 2020;9(9):2942. doi:[10.3390/jcm9092942](https://doi.org/10.3390/jcm9092942)
86. Johansson C, Kirsebom FCM. Neutrophils in respiratory viral infections. *Mucosal Immunol.* 2021;14(4):815-827. doi:[10.1038/s41385-021-00397-4](https://doi.org/10.1038/s41385-021-00397-4)

## SUPPORTING INFORMATION

Additional supporting information can be found online in the Supporting Information section at the end of this article.

**How to cite this article:** Kasumba DM, Huot S, Caron E, et al. DUOX2 regulates secreted factors in virus-infected respiratory epithelial cells that contribute to neutrophil attraction and activation. *The FASEB Journal.* 2023;37:e22765. doi:[10.1096/fj.202201205R](https://doi.org/10.1096/fj.202201205R)